

CLOSER LOOK AT THE TRANSFERABILITY OF ADVERSARIAL EXAMPLES: HOW THEY FOOL DIFFERENT MODELS DIFFERENTLY

Futa Waseda^{1,2}, Sosuke Nishikawa^{1,2}, Trung-Nghia Le², Huy H. Nguyen^{2,3}, and Isao Echizen^{1,2,3}

¹The University of Tokyo, Japan ²National Institute of Informatics, Tokyo, Japan

³The Graduate University for Advanced Studies, SOKENDAI, Kanagawa, Japan

Email: {futa-waseda, nishikawa-sosuke}@g.ecc.u-tokyo.ac.jp, {ltnghia, nhhuuy, iechizen}@nii.ac.jp

ABSTRACT

Deep neural networks are vulnerable to adversarial examples (AEs), which have adversarial transferability: AEs generated for the source model can mislead another (target) model's predictions. However, the transferability has not been understood from the perspective of to which class target model's predictions were misled (i.e., class-aware transferability). In this paper, we differentiate the cases in which a target model predicts the same wrong class as the source model ("same mistake") or a different wrong class ("different mistake") to analyze and provide an explanation of the mechanism. First, our analysis shows (1) that same mistakes correlate with "non-targeted transferability" and (2) that different mistakes occur between similar models regardless of the perturbation size. Second, we present evidence that the difference in same and different mistakes can be explained by non-robust features, predictive but human-uninterpretable patterns: different mistakes occur when non-robust features in AEs are used differently by models. Non-robust features can thus provide consistent explanations for the class-aware transferability of AEs.

Index Terms— deep learning, adversarial examples, transferability, non-robust features

1. INTRODUCTION

Deep neural networks (DNNs) are vulnerable to adversarial examples (AEs), which are slightly perturbed by noises or patterns to mislead DNNs when making predictions [1, 2]. Since AEs can fool DNNs without affecting human perception, they have become a serious threat to real-world DNN applications. The main property of AEs that increases this threat is their transferability: AEs generated using the source model may also fool other models [1, 2, 3]. This transferability enables attackers to use a substitute model to generate AEs that may also fool other unknown (target) models with different architectures or weights (i.e., a "black-box attack" [3]). Therefore, understanding the transferability mechanism has become important for improving the robustness against black-box attacks.

Many studies [1, 2, 3, 4, 5] have investigated adversarial transferability. They can be divided into two categories, i.e., non-targeted and targeted transferability, in accordance with the objective of the adversarial attack. Those were evaluated in a binary way: whether the AE met the attacker's objective or not. Previous studies focused mainly on explaining transferability for non-targeted transferability by using the similarity between the source model and the target model [2, 5, 6, 7].

In contrast, there has been little investigation of transferability from the perspective of to which class target model's predictions were misled, which we refer to as class-aware transferability. In other words, there is a gap between the existing understanding of

- Prediction based on AE with original label "cat"



F1: Source model	×: "dog"		
F2: Target model	○: "cat"	×: "frog"	×: "dog"
Non-targeted transferability	Non-transferable	Transferable	
Targeted transferability (target class: "dog")	Non-transferable		Transferable
Class-aware transferability	Un-fooled	Different mistake	Same mistake

Fig. 1. An example case of classifying the transferability of adversarial example (AE). When an AE generated for the source model fooled it as "dog", the class-aware transferability of the AE is classified into three cases: the target model correctly classifies the AE as "cat" (un-fooled), it misclassifies the AE as "frog" (different mistake) or it misclassifies the AE as "dog" (same mistake). Non-targeted and targeted transferability are defined in a binary way: whether the AE met the attackers' objective or not.

transferability and class-aware transferability. A few studies have revealed one of the properties of class-aware transferability, i.e., that different models tend to make the same wrong predictions for the same AEs (i.e., the "same mistake" effect) [2, 5]. However, the factors that affect the proportion between same mistakes and other cases have not been extensively investigated. Therefore, the mechanisms that cause models to make the same or different wrong predictions for the same AEs have not been clearly explained.

To address this gap, in our research, we first conducted a thorough analysis of class-aware transferability. Second, we tested our hypothesis to comprehensively explain the transferability phenomenon.

First, we analyzed class-aware transferability by evaluating several adversarial attacks, (1) while gradually increasing the difference between the source model and the target model; (2) while gradually increasing the size of the perturbation. We define class-aware transferability by classifying the effect of an AE that fools the source model into three cases: if the target model classifies the AE as the true class, the case is "un-fooled"; if it classifies it as a different wrong class than the source model, the case is "different mistake"; and if it classifies it as the same wrong class as the source model, the case is "same mistake" (illustrated in Fig. 1). We mainly show three points: (1) different mistakes exist even between the source and target models with very high similarity; (2) the tendency for AEs to cause same mistakes has a strong connection with non-targeted

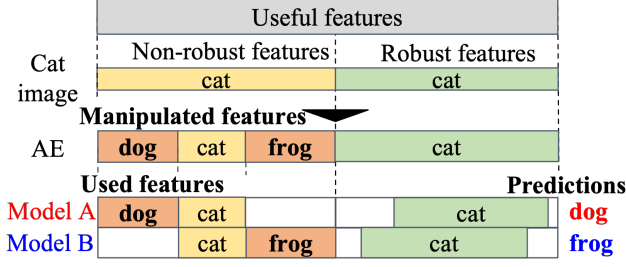


Fig. 2. Our hypothesis on the mechanism of how AEs can cause different predictions for different models. It can happen when non-robust features [7] manipulated by adversarial attacks are differently used by models, due to the model dependency of learning features. For example, even if an AE has both “dog” and “frog” non-robust features, the Model-A may not use much of the “frog” non-robust features and is influenced more by the “dog” non-robust features, and vice versa for the Model-B. Our work extends the findings of Ilyas et al. [7] to allow non-robust features to thoroughly explain both “different mistakes” and “same mistakes.”

transferability; (3) larger perturbations can increase the tendency for AEs to cause same mistakes, while the ratio of different mistakes remains almost constant, indicating that there is the misalignment between the ability of AEs to fool a source model towards a specific class and the ability of AEs to fool a target model towards a specific class that cannot be resolved simply by enlarging perturbations.

Second, to provide a comprehensive explanation of the mechanism of causing a different mistake and a same mistake, we particularly aim to extend the theory of “non-robust features” proposed by Ilyas et al. [7]: AEs can have predictive but human-imperceptible features (i.e., non-robust features), which can strongly affect the predictions of neural networks. They showed that AEs have the non-robust features of the class to which the model was misled. Same mistakes are the logical consequence of their theory: however, there is no evidence that it can also explain a different mistake. We present evidence that AEs that cause different wrong predictions for different models can have the non-robust features of the two different classes to which those models were misled. It indicates that the model dependency of learning features can cause a different mistake: when the manipulated non-robust features in an AE are used differently by multiple models, those models may classify the AE differently (Fig. 2). By strengthening the theory of non-robust features [7], we also support the claim that AEs are at least partly a consequence of “shortcut learning” [8].

Our contributions are summarized as follows,

- Our evaluation of class-aware transferability shows (1) that different mistakes occur even between source and target models with very high similarity and (2) that same mistakes are strongly connected to non-targeted transferability and (3) that larger perturbations do not reduce the ratio of different mistakes, indicating the misalignment in fooling the source and target model towards the same class.
- We provide an explanation of the mechanism causing different and same mistakes by extending the theory of non-robust features. Same mistakes are due to AEs having the non-robust features of the class to which the model was misled. On the other hand, when the manipulated non-robust features in an AE are differently used by different models, those models may classify the AE differently.

2. RELATED WORK

Non-targeted adversarial transferability defines the transferability of AEs by whether or not the target model assigns any wrong class than the true (original) class. Many studies have shown the nature of non-targeted transferability. Szegedy et al. [1] showed that AEs transfer even when the source and target models have different architectures or are trained on a disjoint dataset. Papernot et al. [3] showed that non-targeted AEs transfer even between different machine learning methods such as DNNs, SVMs, and decision trees. Although these studies have shown the intriguing possibility of the transferability, it is unclear how such AEs actually affect the target model’s predictions. In this paper, we analyze class-aware transferability that differentiates a different mistake and a same mistake.

The transferability of non-targeted adversarial attacks has been explained by the similarity between the source and target models. Goodfellow et al. [2] showed that adversarial perturbations are highly aligned with the weight vectors of a model and that different models learn similar functions when trained to perform the same task. Liu et al. [5] revealed by visualization that transferability can arise from the similarity of the decision boundary that separates the true class and other classes. Tramer et al. [6] asserted that transferability appears when “adversarial subspaces” intersect between different classifiers. Ilyas et al. [7] showed that adversarial vulnerability can arise from non-robust features that are predictive but uninterpretable by humans and that transferability arises from the similarity of learned non-robust features between models. However, these explanations do not clearly explain why and when similar models can both be fooled but still have a non-trivial proportion of different mistakes. In this study, we extend the theory of non-robust features to fill this gap.

Targeted adversarial transferability defines the transferability of AEs by whether or not the target model assigns the same specific class as the target class that the source model was attacked towards. Liu et al. [5] showed that, in contrast to non-targeted attacks, targeted attacks rarely transfer between models. Our metrics of class-aware transferability enable us to directly compare the effect of non-targeted and targeted AEs.

Few studies have explained why AEs can cause same mistakes that are directly related to the targeted transferability. Goodfellow et al. [2] hypothesized that it is because of the linear behavior of neural networks. Such behavior is acquired by generalizing to solve the same task and thus resembles a linear classifier trained on the same data. Ilyas et al. [7] provided a widely accepted explanation: models can assign the same class by looking at similar non-robust features in AEs. However, these do not explain our observation that different mistakes occur even between very similar models regardless of the perturbation size. In our study, we aim to extend the theory of non-robust features to clearly explain both different mistakes and same mistakes.

3. ADVERSARIAL TRANSFERABILITY ANALYSIS

3.1. Overview

In this section, we evaluate class-aware transferability of AEs, which differentiates the cases of whether a target model outputs a different wrong class (different mistakes) or the same wrong class (same mistakes) as the source model. We aim to analyze what factors can affect class-aware transferability.

We first evaluate the effect of the model’s factors by gradually changing the similarity between the source and target models. Different from Liu et al. [5], we not only compare models from multiple architectures, but also compare models with different or the same initialized weights and models that are only in different epochs of

training. In addition, we use the quantitative measurement of the distance between the models' decision boundaries devised by Tramer et al. [6] to have a quantitative comparison.

Second, we evaluate class-aware transferability by gradually increasing the perturbation size. Here we aim to analyze how the perturbation size can alter the class-aware transferability of AEs.

3.1.1. Measurement of the transferability

We classify transferability into three cases: whether the target model was "un-fooled," whether the target model made a "different mistake," and whether the target model made a "same mistake." The term "same mistake" was mentioned by Liu et al. [5], which was not the focus of their study.

The focus of our study is to evaluate how the malicious effect of AEs generated for the source model $F1$ can affect the classification results of the (unknown) target model $F2$: we evaluate the distribution of effects of AEs, rather than the adversarial accuracy. Therefore, we evaluate the transferability only for the set of AEs, D'_{F1} , that were able to fool the source model $F1$:

$$(x', y, y1) \sim D'_{F1} = \left\{ (x, y) \sim D \mid \begin{array}{l} F1(x) = y, \\ F1(x') = y1, (\neq y), \end{array} \right\} \quad (1)$$

where AE $x' = \text{adv}(x, y, F1)$ is generated by an adversarial attack $\text{adv}(\cdot)$ on the image-label pair (x, y) from the original set D , and $y1$ denotes the wrong class that the source model misclassified. For these AEs, we define the metrics for class-aware transferability as follows.

1. Un-fooled ratio: $\mathbf{P}_{(x', y, y1) \sim D'_{F1}} [F2(x') = y]$
2. Fooled ratio: $\mathbf{P}_{(x', y, y1) \sim D'_{F1}} [F2(x') \neq y]$
 - (a) Different mistake ratio:
 $\mathbf{P}_{(x', y, y1) \sim D'_{F1}} [F2(x') = y2 (\neq y, \neq y1)]$
 - (b) Same mistake ratio:
 $\mathbf{P}_{(x', y, y1) \sim D'_{F1}} [F2(x') = y1]$

If the target model $F2$ classifies AE x' as the true class y , it is un-fooled; if it classifies it as a different wrong class, $y2$, than source model $F1$, it makes a different mistake; if it classifies it as the same wrong class, $y1$, as source model $F1$, it makes a same mistake.

Note that the fooled ratio corresponds to non-targeted transferability. The same mistake ratio corresponds to targeted transferability only if $y1$ is restricted to the target class of a targeted attack.

3.1.2. Generation of adversarial examples

We examine both non-targeted attacks, which aim to fool a model, and targeted attacks, which aim to fool a model and lead it towards a specific target class y^{tar} . The optimization problems are formulated as

$$(\text{Non-targeted:}) \quad \arg \max_{x'} L(x', y) \quad (2)$$

$$(\text{Targeted:}) \quad \arg \min_{x'} L(x', y^{tar}) \quad (3)$$

where $L(\cdot)$ is the loss function, x' the AE generated from the original input x . Both problems are subject to a l_p -bound, $\|x' - x\|_p < \epsilon$, so that x' remains sufficiently close to x .

We generate AEs by using two gradient-based attacks: (1) one based on the fast gradient method (FGM), which is an efficient method for generating l_p -bounded AEs (the generalized version of the fast gradient sign method (FGSM) [2]) and (2) one based on the projected gradient descent (PGD) method [9], which is the iterative version of FGM that generates stronger AEs for the source model.

3.1.3. Measurement of the similarity of models

For quantitative measurement of the similarity between the source and target models, we use a method devised by Tramer et al. [6]. It measures the average distance of the decision boundary for N images between two models:

$$\text{Dist}(F1, F2) = \frac{1}{N} \sum_i |d(F1, x_i) - d(F2, x_i)| \quad (4)$$

where $d(f, x) = \arg \min_{\epsilon} [f(x + \epsilon \cdot v) \neq y]$ is the minimum distance from an input x to the decision boundary of model f . The distance is calculated in the direction of vector $v = \frac{\nabla_x L(x, y; F1)}{\|\nabla_x L(x, y; F1)\|_2}$, which is a normalized vector of the non-targeted adversarial perturbation generated for the source model $F1$. Therefore, this metric is directly related to the non-targeted transferability.

Since the minimum distance $d(f, x)$ is defined only for a correctly classified image x , we randomly chose 5,000 images from the test set that were correctly classified by all models compared in our experiments and averaged the distances over those images (eq. 4).

3.2. Evaluation settings

Dataset. We used the CIFAR-10 dataset [10]: all models were trained on 50,000 images in the training set, and AEs were generated for 10,000 images in the test set. The generated AEs were l_2 -bounded by the specific ϵ . The PGD-based attacks were iterated for 10 steps with the step size $\alpha = \epsilon/5$. For generating the targeted AEs, a target class for each image was chosen randomly so that there was no correlation between the original labels.

Models. We examined models with five different architectures: ResNet-18, ResNet-34, VGG-16, VGG-19, and DenseNet-121. The optimizer used for training was stochastic gradient descent (SGD) with a momentum of 0.9 and weight decay of 0.0005. The models were trained at an initial learning rate of 0.01, which decayed 0.1 times at the 50th epoch, with 100 epochs in total. For the precise analysis, we independently trained three models for each architecture: two models trained using the same initial weight parameters and one trained using the other initial weights (when the initial weights are the same between models with the same architecture, the only difference is the randomness of the shuffled training data or the dropout layers). In addition, early versions of the source model were also compared as target models at the 80th epoch. Here and after, models $F2$ with "(w:same)" or "(w:diff)" in their name are the models independently trained using the same or different initial weights as used for $F1$; "(v: 80)" is $F1$ at the 80th epoch ($F1$ was trained for 100 epochs).

3.3. Results & discussion

Fig. 3 shows the evaluation results of attacks by FGM and PGD (10 steps) on $F1$: ResNet-18 and $F1$: VGG-16 with both non-targeted and targeted objectives. The order of the target models $F2$ is sorted by $\text{Dist}(F1, F2)$ for each $F1$. The quantitative similarity measurement $\text{Dist}(F1, F2)$ roughly corresponds to the qualitative similarity of the models; for example, when $F1$ was ResNet-18, $F2$ for the ResNet family have shorter $\text{Dist}(F1, F2)$ than other models. We confirmed that both the qualitative and quantitative similarity of the source and target models are positively correlated with the fooled ratio (the sum of different and same mistake ratios), which is consistent with Wu et al.'s observation that non-targeted adversarial transferability is higher between models with similar architectures [11] and the assertion by Tramer et al. that the metric $\text{Dist}(F1, F2)$ is directly related to non-targeted adversarial transferability [6].

First, although the same mistake ratio is the majority of the fooled ratio as reported [2, 5], we observed a non-trivial proportion

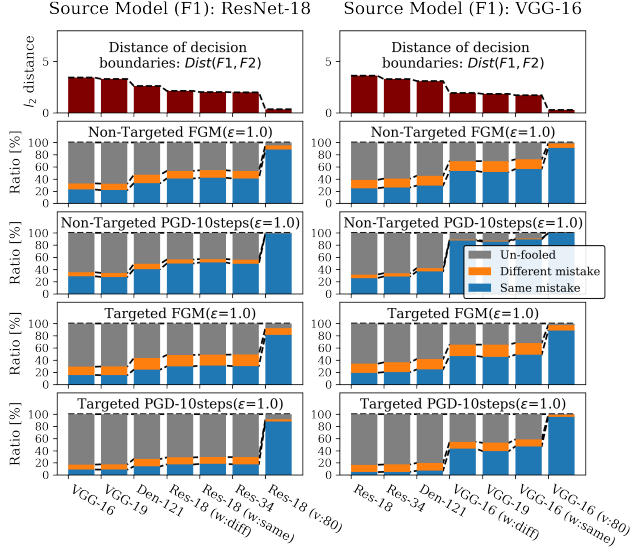


Fig. 3. Class-aware transferability of adversarial attacks against ResNet-18 (left column) and VGG-16 (right column). AEs were l_2 -bounded by $\epsilon=1.0$. The order of F_2 is sorted by $Dist(F_1, F_2)$ (1st row) for each F_1 , so that F_2 that is more to the right in the figure is estimated to be more similar to F_1 .

of different mistakes, even the source and target models are qualitatively very similar (Fig. 3); Even when the models are the same architecture and trained using the same initial weights, the different mistake ratios of targeted FGM were around 20%. Moreover, even the models with only a 20-epoch difference with the smallest $Dist(F_1, F_2) < 0.5$ had 10% of different mistake ratio when attacked by targeted FGM. This result raises the question of what can explain the existence of different mistakes between such similar models, which we address in the later section.

Second, we observed that the same mistake ratio strongly correlates with the fooled ratio (Fig. 3). Similar to the fooled ratio, the same mistake ratio is higher when the source and target models are in the same architecture family (e.g., ResNet-18 and ResNet-34 are both in the ResNet family), and when the target models are just the early version of the source model. The correlations between the fooled ratio and the same mistake ratio were above 0.98, and the correlations between $Dist(F_1, F_2)$ and the same mistake ratio were under -0.90 in all 8 cases in Fig. 3. These correlations show that non-targeted transferability of AEs and the tendency of AEs to cause same mistakes have a strong connection.

Third, while a larger perturbation can enable AEs to have a stronger effect to cause same mistakes, the different mistake ratio stays almost constant or increase (Fig. 5). This indicates that there is the misalignment between the ability of AEs to fool the source model towards a specific class and the ability of AEs to fool the target model towards a specific class that cannot be resolved simply by enlarging perturbations.

To further interpret these observations, we visualized the decision boundaries, as in Liu et al. [5] (Fig. 4). We chose two directions of δ_1 , the non-targeted gradient direction of ResNet-18, and δ_2 , the random orthogonal direction. Both δ_1, δ_2 are normalized to 0.02 by l_2 -norm. Each point (u, v) in the 2-D plane corresponds to the image $x + u\delta_1 + v\delta_2$, where x is the source image. For each model, we plot the classified label of the image corresponding to each point. First,

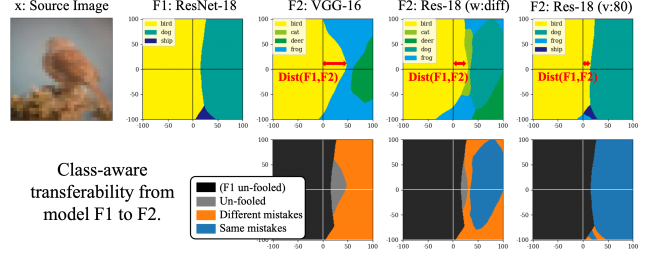


Fig. 4. Visualization of decision boundaries for the source image of “bird”, as in Liu et al. [5]. The first row shows the classification results, where each color represents a certain class. The second row shows to which area the three cases of class-aware transferability corresponds. The distance from (0,0) point to the closest decision boundary along x-axis corresponds to the metric $Dist(F_1, F_2)$ for this single image. The unit of each axis is 0.02 in l_2 distance.

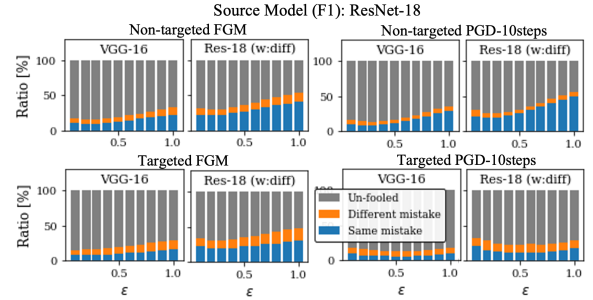


Fig. 5. Class-aware transferability of AEs when the size of perturbation ϵ is gradually changed.

we see that the area of different mistakes exist between the models with the same architecture or even models with only a 20-epoch difference. On the other hand, we see that when the distance from the original source image to the closest decision boundary along the x-axis ($=Dist(F_1, F_2)$) is smaller, the area of the same mistake is larger. Liu et al. [5] showed that non-targeted transferability arises from the similarity of the decision boundary that separates the true class and other classes, on the other hand, our results further show that when the decision boundaries that separate the true class and other classes are similar between two models, the decision boundaries that separate wrong classes can also be similar between the models, resulting in the correlation between fooled ratio and same mistake ratio.

The observed strong connection between non-targeted transferability and the same mistakes supports the existence of non-robust features [7] in AEs: AEs can cause same mistakes by having non-robust features that correlate with a specific class. However, the consistent existence of different mistakes between very similar models or when the perturbations are large has not been understood. We hypothesized that different mistakes can happen because the usage of non-robust features are model-dependent, which we test in the later section.

4. NON-ROBUST FEATURE INVESTIGATION

4.1. Overview

Here we provide the first possible explanation for different mistakes, which can also explain same mistakes. Specifically, we aim to ex-

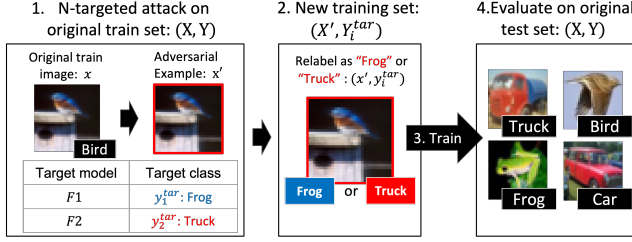


Fig. 6. Illustration of experiment in Section 4 to test our hypothesis that a different mistake can arise from AEs having non-robust features of two different classes to which two different models were misled (Fig. 2). First, original training set is attacked by the N-targeted attack. Next, a new (non-robust) dataset is constructed by relabeling generated AEs as either Y_1 or Y_2 , the target classes for F_1 or F_2 . Finally, a model is trained on new dataset and evaluated on original test set.

tend the theory of non-robust features [7]. Same mistakes can be interpreted as the result of different models using similar non-robust features; we present evidence that a different mistake can also arise from non-robust features.

We generate AEs that can cause different mistakes for different models, and by extending Ilyas et al.’s experiment [7], we show that those AEs have non-robust features of two different classes to which those models were misled. This means that the two models did different predictions on the same AEs since they had biases on using the non-robust features of those two classes. Therefore, we conclude that the theory of non-robust features can comprehensively explain different and same mistakes: Same mistakes are due to AEs having the non-robust features of the class to which a model was misled; on the other hand, AEs may have multiple non-robust features that correlate to different classes at the same time, and if models differently use them, the models may classify the same AEs differently (Fig. 2).

Experiment. We tried to detect non-robust features of two different classes from the AEs that cause different mistakes. If those AEs have the non-robust features of the two misleading classes at the same time, we can assume that the non-robust features were used differently by the models (as in Fig. 2). To show the existence of non-robust features in AEs, we use the framework for non-robust features described by Ilyas et al. [7]. We extend their experiment to detect non-robust features of two wrong classes, whereas Ilyas et al. [7] did it with only one wrong class.

The flow of the experiment is illustrated in Fig. 6. First, we attacked two models, F_1 and F_2 , in a white-box setting that both models are accessible in attacks, on the original training set to generate AEs that can cause different mistakes for each model (F_1 is misled to classes Y_1 and F_2 to classes Y_2 for the original images X). Then, we created new (non-robust) training sets using two ways of relabeling the AEs, i.e., by either of the target classes Y_1 or Y_2 . Finally, we trained a model on the new training set ($D'_1 : (X', Y_1)$ or $D'_2 : (X', Y_2)$) and evaluated it on the original test set, $D : (X, Y)$. If both non-robust sets $D'_1 : (X', Y_1)$ and $D'_2 : (X', Y_2)$ were useful in generalizing to the original set, we can conclude that non-robust features of both classes of Y_1 and Y_2 exist in the same AEs at the same time.

We generated AEs that can cause different mistakes for F_1 and F_2 by using our extended version of a targeted attack, namely *N-targeted attack*. This attack is aimed at fooling model F_i to lead it towards each target class y_i^{tar} . The objective of an N-targeted attack

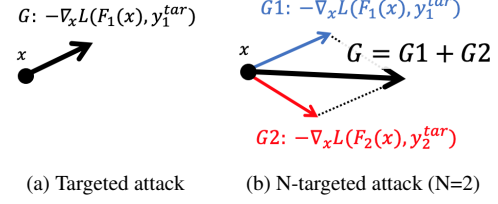


Fig. 7. Update gradient G for gradient-based (a) targeted attack and (b) proposed N-targeted attack ($N=2$). N-targeted attack sums up all gradients for all targeted models ($G = G_1 + G_2$) and aims to fool a model F_1 and lead it towards a class y_1^{tar} and lead a model F_2 towards a class y_2^{tar} .

Original										
Adversarial (N-targeted attack)										
True Label	Plane	Car	Bird	Cat	Deer	Dog	Frog	Horse	Ship	Truck
Pred: Res-18	Truck	Frog	Cat	Frog	Bird	Plane	Deer	Deer	Dog	Ship
Pred: VGG-16	Deer	Frog	Frog	Ship	Horse	Truck	Car	Plane	Dog	Bird

Fig. 8. Examples of AEs (lower row) generated for the images from CIFAR-10 [10] (upper row) by N-targeted attack that was l_2 -bounded by $\epsilon=1.0$ (best viewed online in color with zoom-in). The table shows the true labels and the predictions on the AEs by models. The original images above were all correctly classified by both ResNet-18 and VGG-16, while the AEs fooled ResNet-18 and led it towards classes Y_1 and VGG-16 towards classes Y_2 , where Y_1 and Y_2 are the two different sequences of a randomly selected class for each image. Confidence values for shown AEs were all above 99%, indicating successful attacks by N-targeted attack. The entire set of generated AEs comprises a non-robust set, with relabeling of AEs by either Y_1 or Y_2 .

is described as

$$\arg \min_{x'} \sum_i^N L(F_i(x'), y_i^{tar}), \text{ s.t. } \|x' - x\|_p < \epsilon. \quad (5)$$

It simply sums up all loss values for all targeted models. The optimization problem is iteratively solved by using the same algorithm used for PGD [9]. The difference between an N-targeted attack and a normal targeted attack is illustrated in Fig. 7. The generated AEs for $\{F_1, F_2\} = \{\text{ResNet-18, VGG-16}\}$ are shown in Fig. 8.

Non-robust set constructed for		F1(X') = Y_1	F2(X') = Y_2	F1(X')= Y_1 & F2(X')= Y_2
F1	F2			
Res-18	VGG-16	95.6	99.0	95.4
Res-18	Res-18 (w: same)	94.1	94.1	92.0
VGG-16	VGG-16 (w: same)	99.5	99.5	99.2

Table 1. Accuracy of attacked models on AEs X' generated by using N-targeted attack, which constructs non-robust sets. Y_1 is the target classes for N-targeted attack for the model F_1 , and Y_2 for the model F_2 . These results are particularly interesting: in a white-box setting, it is easy to generate AEs that lead to different sequences of class Y_1 and Y_2 (success rate $> 90\%$).

4.2. Experiment settings

Construction of non-robust set was done by N-targeted attack based on PGD-based optimization with l_2 -bound of $\epsilon=0.1$, step size

Non-robust set constructed for	Trained label	Trained model	Test acc (X,Y)
F1: Res-18 F2: VGG-16	Y1	Res-18	51.3
		VGG-16_bn	53.9
	Y2	Res-18	10.2
		VGG-16_bn	71.0
F1: Res-18 F2: Res-18 (w:same)	Y1	Res-18	50.1
		VGG-16_bn	54.1
	Y2	Res-18	59.2
		VGG-16_bn	58.9
F1: VGG-16 F2: VGG-16 (w:same)	Y1	Res-18	63.5
		VGG-16_bn	68.8
	Y2	Res-18	11.0
		VGG-16_bn	73.1

Table 2. Test accuracy on original test set when trained on non-robust sets. Each set was labeled with either Y1 or Y2, the target classes of N-targeted attack for models F1 and F2. Test accuracy when trained on the original training set was 88% for ResNet-18 and 93% for VGG-16.bn. Since random accuracy is 10% for 10-class classification task, we confirmed that the models generalized to the original test set by training on non-robust sets. Interestingly, non-robust sets were relabeled either by two unrelated class sequences of Y1 or Y2 that both appear to be completely random (Fig. 8).

$\alpha=0.1$, 100 steps. Target classes Y1 and Y2 were randomly chosen for every data point, so that relabeled labels did not correlate with the original classes (note that each target class y_1^{tar} and y_2^{tar} can be the same class or the original class). Non-robust datasets were constructed for {F1, F2}={ResNet-18, VGG-16} (a model pair with different architectures) and {ResNet-18, ResNet-18 (w:same)}/{VGG-16, VGG-16 (w:same)} (a model pair with the same architecture and initial weights), the same models used in the analysis described in Section 3. Note that for all non-robust sets, the ratios of the models F1/F2 fooled and led towards the classes Y1/Y2 at the same time were over 90%, which means that the N-targeted attack successfully generated AEs that lead the two models towards the different sequences of class Y1 and Y2 (Table. 1).

Training models on non-robust data. The optimizer was SGD set to momentum = 0.9 and weight decay = 0.0005, similar to the normal case. The learning rate decayed 0.1 times at the 100th and 150th epoch, with training for 200 epochs. The initial learning rate, batch size, and data augmentation were optimized by using a grid search. The models used were ResNet-18 and VGG-16.bn (VGG-16 with batch normalization).

4.3. Results & discussion

The test accuracies of the models trained on the constructed non-robust sets are shown in Table 2. For all three pairs of attacked models F1 and F2, the test accuracies on the original test set (X, Y) were very high for both cases of relabeling by Y1 or Y2. In most cases, high test accuracy was achieved both when training ResNet-18 and VGG-16 (with batch normalization). It means that the models could learn non-robust features of Y1 by training on non-robust set (X', Y1) and also non-robust features of Y2 by training on non-robust set (X', Y2). Therefore, we confirm that the generated AEs X' have multiple non-robust features that correlate with two different classes at the same time, supporting our hypothesis: when the manipulated non-robust features in an AE are differently used by models, those models may classify the AE differently. The reason that different mistakes do not decrease with the increase of the perturbation size can be that the size of perturbations does not necessarily solve the misalignment of the different usage of non-robust

features between models. Therefore, together with the strong connection between non-targeted transferability and same mistakes observed in Section 3, which is consistent with the existence of non-robust features of a specific class in AEs, we conclude that non-robust features can comprehensively explain both different and same mistakes.

In addition, we observed the model dependency of learning non-robust features even between models with the same architecture and trained using the same initial weight parameters. This suggests that learning non-robust features can be quite random when the models are trained using the SGD optimizer (and additionally the dropout layers in VGG models) due to the stochasticity of updating the weight parameters. The reason that a non-trivial proportion of different mistakes exist between models with high similarity in Section 3 can be that stochasticity in training has a large effect on learning non-robust features.

5. CONCLUSION

Our analysis on class-aware transferability first showed the strong connection between non-targeted transferability of AEs and same mistakes. This is consistent with the claim that AEs can have non-robust features that correlate with a certain class to which models can be misled. However, we further showed that different mistakes occur between very similar models regardless of the perturbation size, which raises the question how AEs cause different mistakes.

We demonstrated that non-robust features can comprehensively explain the difference between a different mistake and a same mistake by extending the framework for non-robust features described by Ilyas et al. [7]. They showed that AEs can have non-robust features that are predictive but human-imperceptible, which can cause a same mistake. In contrast, we showed that when the manipulated non-robust features in an AE are differently used by multiple models, those models may classify the AE differently.

Future work includes analyzing class-aware transferability for not only basic attack methods and models but also state-of-the-art ones with the aim of strengthening the understanding of class-aware transferability. In addition, since we cannot conclude that our explanation by non-robust features is consistent for *all* different mistakes, whether there is another mechanism or not is an important research question.

6. REFERENCES

- [1] Christian Szegedy, Wojciech Zaremba, Ilya Sutskever, Joan Bruna, Dumitru Erhan, Ian Goodfellow, and Rob Fergus, "Intriguing properties of neural networks," in *ICLR*, 2014.
- [2] Ian J Goodfellow, Jonathon Shlens, and Christian Szegedy, "Explaining and harnessing adversarial examples," in *ICLR*, 2015.
- [3] Nicolas Papernot, Patrick McDaniel, and Ian Goodfellow, "Transferability in machine learning: from phenomena to black-box attacks using adversarial samples," *arXiv preprint arXiv:1605.07277*, 2016.
- [4] Yinpeng Dong, Qi-An Fu, Xiao Yang, Tianyu Pang, Hang Su, Zihao Xiao, and Jun Zhu, "Benchmarking adversarial robustness on image classification," in *CVPR*, 2020, pp. 321–331.
- [5] Yanpei Liu, Xinyun Chen, Chang Liu, and Dawn Song, "Delving into transferable adversarial examples and black-box attacks," in *ICLR*, 2017.
- [6] Florian Tramèr, Nicolas Papernot, Ian Goodfellow, Dan Boneh, and Patrick McDaniel, "The space of transferable adversarial examples," *arXiv preprint arXiv:1704.03453*, 2017.
- [7] Andrew Ilyas, Shibani Santurkar, Dimitris Tsipras, Logan Engstrom, Brandon Tran, and Aleksander Madry, "Adversarial examples are not bugs, they are features," in *NeurIPS Reproducibility Challenge*, 2019.
- [8] Robert Geirhos, Jörn-Henrik Jacobsen, Claudio Michaelis, Richard Zemel, Wieland Brendel, Matthias Bethge, and Felix A Wichmann, "Shortcut learning in deep neural networks," *Nature Machine Intelligence*, vol. 2, no. 11, pp. 665–673, 2020.

- [9] Aleksander Madry, Aleksandar Makelov, Ludwig Schmidt, Dimitris Tsipras, and Adrian Vladu, "Towards deep learning models resistant to adversarial attacks," in *ICLR*, 2018.
- [10] Alex Krizhevsky and Geoffrey Hinton, "Learning multiple layers of features from tiny images," Tech. Rep., University of Toronto, 2009.
- [11] Lei Wu, Zhanxing Zhu, and Tai, "Towards understanding and improving the transferability of adversarial examples in deep neural networks," *ACML*, 2020.